



Differential gene expression between normoxic and hypoxic conditions in the moon jellyfish *Aurelia coerulea* (Scorrano)

Y Xing^{a,c} & G Wang^{*,b}

^aGuangxi Academy of Sciences, Guangxi Mangrove Research Center, Guangxi Key Lab of Mangrove Conservation and Utilization, Beihai – 536 007, P. R. China

^bNational Marine Hazard Mitigation Service, Ministry of Natural Resources, Beijing – 100 194, P. R. China

^cKey Laboratory of Tropical Marine Ecosystem and Bioresource, Fourth Institute of Oceanography, Ministry of Natural Resources, Beihai – 536 000, P. R. China

*[E-mail: wangguoshan2013@126.com]

Received 08 May 2020; revised 20 February 2022

Compared with other marine organisms, jellyfish are tolerant to hypoxia and frequently occur in minimum oxygen zones. However, the molecular mechanisms underlying this tolerance remain unknown. This study investigated the molecular mechanisms responsible for hypoxia tolerance in *Aurelia coerulea* by cultivating them in an enclosed cultivation system under hypoxic and oxygen-saturated conditions for 18 h, followed by transcriptome-wide RNA sequencing (RNA-Seq). Differential expression analysis indicated that 417 unigenes in medusae and 202 unigenes in polyps were differentially expressed between hypoxic and oxygen-saturated conditions. These differentially expressed genes were mainly involved in the metabolic process and catalytic activity and enriched in protein digestion and absorption, Hypoxia-Inducible Factor-1 (HIF-1) signalling and oxidative phosphorylation pathways. Some of these specific transcripts in the enriched pathways were validated by quantitative real-time polymerase chain reaction. These results may provide mechanistic insights into the hypoxic tolerance of lower marine invertebrates that absorb oxygen directly from the water.

[**Keywords:** *Aurelia coerulea*, Differential expression, HIF-1 signalling pathway, Hypoxic tolerance, Transcriptome]

Introduction

Huge swarms of jellyfish can seriously affect the stability of coastal marine ecosystems by feeding on zooplankton, fish eggs, and fish larvae, causing major economic and social problems related to tourism, coastal industries, and fishery resources. The dominant species of jellyfish in blooms in Chinese coastal waters include *Nemopilema nomurai*, *Cyanea nozakii*, and moon jellyfish, identified as *Aurelia coerulea* (*Aurelia* sp. 1) by molecular methods based on *COI* and *28S* gene sequences¹. *Aurelia* is one of the most common Scyphomedusae and is famous for its successful invasion of foreign habitats worldwide. Its life cycle involves asexually reproductive polyps and sexually reproductive medusae. The sessile polyps attach tightly to suitable hard substrates, while the pelagic medusae migrate vertically or horizontally with the tides and currents.

Recent reviews speculated that the increase in jellyfish populations may be supported by changes in environmental factors, such as temperature, eutrophication, coastal engineering and marine

minimum oxygen zones^{2,3}. Indeed, the severity, frequency of occurrence, and spatial scale of hypoxia have increased during the past few decades and are expected to become worse in the coming years⁴. Hypoxia affects the survival of most marine organisms and leads to a major loss of biodiversity in marine communities in coastal waters. Numerous studies have demonstrated the tolerance of jellyfish to low oxygen concentrations and characterized the physiological features of polyps and medusae under different hypoxic conditions. Although the bell-contraction rate of moon jellyfish medusae was unaffected by oxygen concentrations within the tested range (1.0, 2.0, 4.0 and 5.8 mg/L)⁵⁻⁷, predation rates were significantly higher at 1.0 and 2.0 mg/L compared with 4.0 and 5.8 mg/L. The median survival of moon jellyfish polyps at 0.28 mg/L oxygen was 120 h and the polyps can normally survive and reproduce at 2.8 mg/L⁸.

Animals have evolved sophisticated mechanisms to maintain cellular oxygen homeostasis, involving up and down-regulating gene expression⁹. Jellyfish lack

respiratory and vascular systems, and oxygen, therefore, enters jellyfish cells by free diffusion from seawater, rather than by active absorption, as in fish and mammals. Changes in dissolved oxygen in seawater, thus, directly affect cellular oxygen homeostasis in jellyfish. Cnidarians, such as jellyfish are therefore, suitable organisms for studying the molecular mechanisms underlying the hypoxia response and tolerance. Wang *et al.*^{10,11} identified an analogue of HIF in *A. coerulea* and showed that the expression of HIF increased at the transcriptional level under hypoxia. Subsequently, the up-regulation of *ALDO*, *PDK* and *LDH*, which was directly or indirectly induced by HIF, mediated the transition from aerobic respiration to anaerobic glycolysis in the medusae stage of *A. coerulea*¹². It is well-known that the molecular regulation mechanism of biological response to environmental stress involves a variety of basic physiological processes. Although it has been confirmed that oxygen homeostasis and energy metabolism are important parts of the molecular regulation mechanism of hypoxia tolerance in *A. coerulea*, there are still many problems that have not been resolved. For example, how do oxygen homeostasis and energy metabolism interact with other biological processes?

Next-generation sequencing technologies have been widely used to identify genes and quantify RNA expression profiles under different experimental conditions. Genes related to ion-transport and energy production were shown to be up-regulated in response to CO₂-driven pH decrease in corals using transcriptome analysis¹³. Elran *et al.*¹⁴ employed a transcriptome-wide RNA sequencing (RNA-Seq) approach to analyze the *Nematostella vectensis* molecular defence mechanisms against four heavy metals and identified co-upregulation of immediate-early transcription factors, including *Egr1*, *API* and *NF-κB*. Hypoxia also significantly affects the movement, feeding, reproduction, and survival of organisms in marine ecosystems¹⁵. Transcriptome analysis was used to investigate low-oxygen adaptability in Crucian Carp (*Carassius auratus*), Plateau Fish (*Triplophysa dalaica*), Sculpins (*Oligocottus maculosus*), Ruffe (*Gymnocephalus cernua*) and Flounder (*Platichthys flesus*) at the molecular level¹⁶⁻¹⁹.

The life cycle of *Aurelia* includes an asexual generation of polyps and a sexual generation of medusae. The sessile polyps attach tightly to suitable hard substrates in certain waters, while the pelagic

medusae can migrate vertically and horizontally in response to tides and currents. These two lifestyles, characterized by rest and exercise, respectively, have very different oxygen requirements and the molecular mechanisms of the respective hypoxia responses may thus also differ. In this study, we analyzed the transcriptomes of *A. coerulea* medusae and polyps and compared their RNA expression profiles under normal and hypoxic dissolved oxygen concentrations. They help to elucidate the molecular regulatory mechanisms acting under hypoxic conditions in jellyfish, and further our understanding of the molecular evolution of aerobic animals.

Materials and Methods

The research was conducted by using the moon jellyfish, *Aurelia coerulea*. Medusae (umbrella diameter about 3.0 cm) and polyps were provided by the Institute of Oceanology, Chinese Academy of Sciences. The polyps were attached to a corrugated polyethylene board and cultured in a 30 L aquarium at the temperature of 20±01 °C, with a natural photoperiod and indoor natural light intensity and fed *Artemia nauplii*. Test seawater was taken from the coastal water of Qingdao, with a salinity of 33 and a pH of 7.5 – 8.0.

Methodology

Conditional culture experiment

Moon jellyfish with an umbrella diameter of about 3.0 cm were fed sufficiently at room temperature (20 °C) for 12 h, and medusae with good activity were then divided into a control group and a hypoxia group (n = 3 each). Medusae were sampled after cultivation for 18h in the culture tank, with each medusa used as an independent sample. Polyps were cultured on a corrugated polyethylene board and fed sufficiently for 12 h before the experiment. Polyethylene blocks (5×5 cm) were cut and polyps that were not growing well on the blocks were discarded. Fifty polyps were retained on each corrugated block for controlled ecological experiments. One polyethylene block with polyps was placed in a control tank and one in a hypoxic culture tank, respectively, and cultivated for 18 h, followed by sampling. The hypoxia culture tank is the same as the description by Wang *et al.*¹². Thirty polyps were picked randomly from each block and divided into three replicates (n = 10 each). The temperature was maintained at 20±01 °C throughout the experiment, and the dissolved oxygen concentration was monitored every 2 h using a Model

HQ30d multi-parameter metre (HACH, Beijing, China).

Extraction and quality measurement of total RNA

Extraction of total RNA from medusae

Medusae were pre-frozen in liquid nitrogen and total RNA was extracted by grinding in liquid nitrogen, lysis with TransZol (TransGen Biotech, Beijing, China), extraction with chloroform/isopropyl alcohol, and washing with 75 % alcohol. The total RNA obtained was dissolved in 50 μ L of DEPC water and stored at -80°C until use. Total RNA extraction was performed according to the TransZol instructions.

Extraction of total RNA from polyps

The total RNA was extracted from polyps following the procedure described by Schroth *et al.*²⁰. The RNA was stored at -80°C until use.

Quality measurement of total RNA

Total RNA integrity and contaminants were detected by 1 % agarose gel electrophoresis, and the concentration and purity of total RNA were determined by Nanodrop 2000 (Thermo Scientific, Massachusetts, America). The RNA concentration was quantified by QubitTM 4 Quantitation Starter Kit (Thermo Scientific, Massachusetts, USA), and its integrity was detected using an Agilent Bioanalyzer 2100 (Agilent Technologies, Inc, Beijing, China).

Preparation of transcriptome sequencing and real-time fluorescence PCR samples

Total RNA from replicate medusa and polyps were respectively divided into two, one for transcriptome sequencing and the other for real-time fluorescent quantitative PCR. Of those, total RNA that used for transcriptome sequencing, were mixed using equal amounts of RNA from three identical biological replicates of different treatment groups. Finally, four total RNA samples including Hypoxia Medusae (HM), Control Medusae (SM), Hypoxia Polyp (HP), and Control Polyp (SP) were obtained. While there were 12 separate total RNA samples for subsequent qPCR amplification.

Library construction and examination

The procedure of Library construction was made according to the NEBNext[®] UltraTM RNA Library Prep Kit for Illumina[®] (NEB, USA). The libraries were subjected to preliminary quantification using Qubit 2.0. The libraries were diluted to 1.5 ng/ μ L, and the insert size was detected using an Agilent 2100 (Agilent Technologies, Inc, Beijing, China).

Library sequencing

Different qualified libraries were pooled according to the effective concentration and target sequence data and sequenced using an Illumina HiSeq system by Novogene Bioinformatics Co., Ltd. (Beijing, China).

Bioinformatics analysis

Within the phylum Cnidaria, no genome sequences are available for Scyphozoa. The moon jellyfish transcriptome could thus only be analyzed using a reference-free transcriptome method, with the assembled transcripts as reference sequences.

Transcript assembly

Clean reads were obtained for the four samples as described above and assembled into contigs with a length of 30 bp and 80 % similarity using Trinity software²¹.

Gene functional annotation

The assembled unigenes were aligned against seven databases: Nr, Nt, Pfam, KOG/COG, Swiss-Prot, Kyoto Encyclopedia of Genes and Genomes (KEGG), and Gene Ontology (GO), and the sequence with the lowest E-value in each database was selected as the annotation result.

Analysis of gene expression levels

The assembled transcripts were used as reference sequences, and the clean reads from the four samples were mapped to the reference sequences using RSEM software²². The read counts mapped to each gene in each sample were then enumerated and normalized using the fragments per kilobase per million mapped fragments (FPKM) method.

Differential gene expression analysis

Differential gene expression data were derived from the read-count data. The read-count data were first normalized by the Trimmed Mean of M value (TMM), and the differences were analyzed by DEGseq (an R package for identifying differentially expressed genes from RNA-seq data). To reduce the false-positive rate of differentially expressed genes, genes with a q value < 0.005 and $|\log_2(\text{fold_change})| > 1$ were screened out. The numbers of common and unique differentially expressed genes in two sample groups (SP vs HP; SM vs HM) were calculated and compared and screened for the following analyses.

GO enrichment analysis

GO-term enrichment is used to determine if a set of genes is overrepresented at a functional node, and can

be used to annotate individual genes and large sets of genes. The number of genes significantly enriched in each GO term was calculated for functional studies of differentially expressed genes.

KEGG enrichment analysis

Different genes coordinate with each other to carry out their biological functions *in-vivo*. The main biochemical metabolic and signalling pathways involving differentially expressed genes can be determined by enrichment analysis of signalling pathways based on KEGG pathways. Signalling pathways significantly enriched in differentially expressed genes relative to all annotated genes were identified by hypergeometric tests.

Quantitative verification of key genes

Design of primers for qPCR

The quantitative primer (Qtubulin YF/YR) of the tubulin gene was obtained from Wang *et al.*¹⁰. The qPCR primers of PHD, ALDO and HSP70 genes are QPHD YF/YR, QALDO YF/YR and QHSP70 YF/YR. Those primers had been verified in Wang *et al.*¹². Primers for collagen, transferrin, hypoxia-inducible factor (HIF)-1 β , CBP/p300, heme oxygenase, NADH dehydrogenase, cytochrome c oxidase and activator protein-1 (AP1) were designed using Primer Premier 6, according to the respective cDNA sequences from RNAseq. Primer sequences are listed in Table S1.

Preparation of cDNA

12 cDNA samples for use in quantitative PCR were obtained using the PrimeScriptTM RT reagent kit with gDNA Eraser (TaKaRa, Dalian, China) from the 12 separate total RNA samples separately.

Detection of target genes by real-time qPCR (RT-qPCR)

qPCR was carried out using FastStart Universal SYBR Green Master (Rox) system (ROCHE, USA) (Table S2). The reaction mixtures were pre-denatured at 95 °C for 10 min, followed by 40 cycles of denaturation at 95 °C for 15 s, annealing and extension at 58 °C for 1 min. Each PCR reaction was repeated three times.

Data analysis

The α -tubulin gene was used as an internal control gene, with the control group as a reference. Relative expression levels of target genes were analyzed by the 2^{- $\Delta\Delta$} Ct method.

Results

Dissolved oxygen concentration profiles

The medusa-hypoxic and polyp-hypoxic groups were maintained at Dissolved Oxygen (DO) concentrations of 0.57 \pm 0.08 (mean \pm SD) and 0.63 \pm 0.06 mg/L throughout the experiment, respectively, whereas the DO concentrations for the control groups were 8.67 \pm 0.06 and 8.72 \pm 0.09, respectively.

RNA quality

The quality of the RNA samples is summarized in Table 1. The RNA samples were not degraded and their integrity was good. The absorbance ratios of the four samples were around 2.0, indicating high purity. The results of the Agilent 2100 test are shown in Figure S1. The quality of the RNA samples met the requirements for library construction and sequencing.

De novo assembly of jellyfish transcriptome and data analysis

The four samples (SP, HP, SM, and HM) were subjected to high-throughput sequencing to obtain raw reads. After removing adapter sequences and low-quality reads, 8.1 Gigabyte (G), 9.7 G, 5.95 G, and 7.38 G clean reads were generated, respectively, and 31.13 G of sequencing data were obtained. The Q20 (≤ 1 % sequencing error rate) values of the four samples were 96.73 %, 96.90 %, 96.09 %, and 96.28 %, respectively, indicating base error rates in the sequencing data of 0.02, 0.01, 0.02, and 0.02, respectively. The GC contents of the four samples were 43.40 %, 43.07 %, 41.63 %, and 41.87 %, respectively, and the average GC content was 42.49 % (Table S3).

Clean reads were obtained for the four samples after filtering, and *de novo* assembly of the clean reads generated transcriptome data containing 176,530 sequences. The longest transcript of each gene in the transcriptome sequences was selected as a unigene, and a total of 138,945 unigenes were obtained for subsequent transcriptome annotation and gene expression analysis. The assembled unigenes had an N50 of 794 bp and an average length of 532 bp

Table 1 — The test results summary of RNA samples

Samples Name	Concentration (ng/ μ L)	OD _{260/280}	OD _{260/230}	28S/18S	RNA Integrity Number (RIN)
SP	698	2.017	2.511	0.9	7.6
HP	742	2.027	2.441	1	8.6
SM	930	1.996	2.246	3.7	8.8
HM	1,288	2.019	2.325	3	9.2

(Fig. 1). N50 is the contig length for which at least 50 % of the assembled transcript nucleotides.

Transcriptome annotation

The assembled unigenes were assigned functional annotations against the seven databases (Table 2). Most unigenes (36,989) were annotated in the GO database (accounting for 26.61 % of the total unigenes), while the fewest unigenes (16,326) were annotated in the KO database (11.74 % of the total unigenes). A total of 55,717 unigenes were annotated, accounting for 40.1 % of the total unigenes.

The annotated unigenes mapped mainly to *H. vulgaris*, *N. vectensis*, *Strongylocentrotus purpuratus*, *Branchiostoma floridae*, and *Crassostrea gigas*, with 6181, 4375, 1011, 1006, and 995 corresponding unigenes, respectively (Fig. 2).

GO annotation

A total of 36,986 GO-annotated unigenes were enriched into corresponding categories (Fig. 3). In the category of biological process, most unigenes

Table 2 — Annotated Unigene number of different databases

Database	Number of unigenes	Percentage (%)
Annotated in NR	36243	26.08
Annotated in NT	18582	13.37
Annotated in KO	16326	11.74
Annotated in SwissProt	31178	22.43
Annotated in PFAM	36343	26.15
Annotated in GO	36986	26.61
Annotated in KOG	21490	15.46
Annotated in all databases	4790	3.44
Annotated in at least one database	55717	40.1
Total unigenes	138945	100

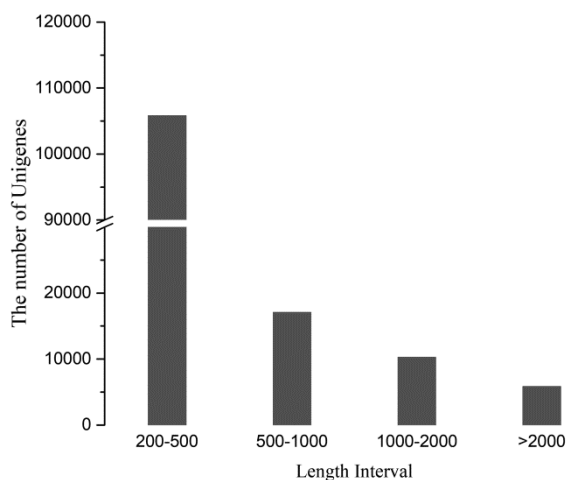


Fig. 1 — Length distribution of unigenes

(20,549; 55.6 %) were related to cellular process, followed by metabolic process (18,386; 49.7 %); in the category of cellular components, most unigenes were associated with the cell (11,355; 30.7 %), followed by cell part (11,354; 30.6 %); and in the category of molecular function, most unigenes (18,651; 50.4 %) were associated with binding, followed by catalytic activity (14,356; 38.8 %).

KEGG classification

A total of 16,326 KO-annotated unigenes were enriched into specific metabolic pathways (Fig. 4), ranked in descending order according to the number of annotated unigenes as follows: translation, signal transduction, transport and catabolism, endocrine system, folding, sorting, and degradation, and carbohydrate metabolism.

Analysis of gene expression levels

In the reference-free transcriptome, genes with an FPKM > 0.3 were considered to be expressed. The distribution of FPKM densities of genes in the four samples exhibited a non-standard normal distribution (Fig. 5a). Genes with FPKM values < 0.3 and > 0.3 accounted for 57.03 % and 42.97 % in the SP sample, 51.43 % and 48.57 % in the HP sample, 57.67 % and 42.33 % in the SM sample, and 58.89 % and 41.11 % in the HM sample, respectively. The median FPKM values in the SP, HP, SM and HM samples were 0, 14.0, 0.21 and 13.2, and the mean FPKM values were 0, 16.4, 0.21 and 22.6, respectively (Fig. 5b).

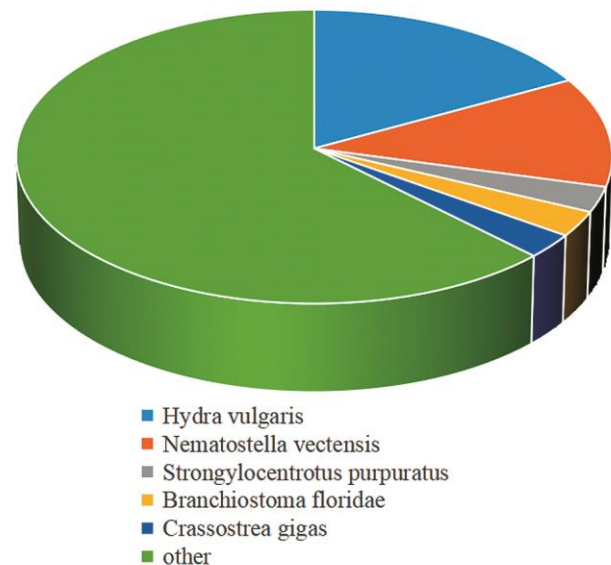


Fig. 2 — The species of annotated unigenes

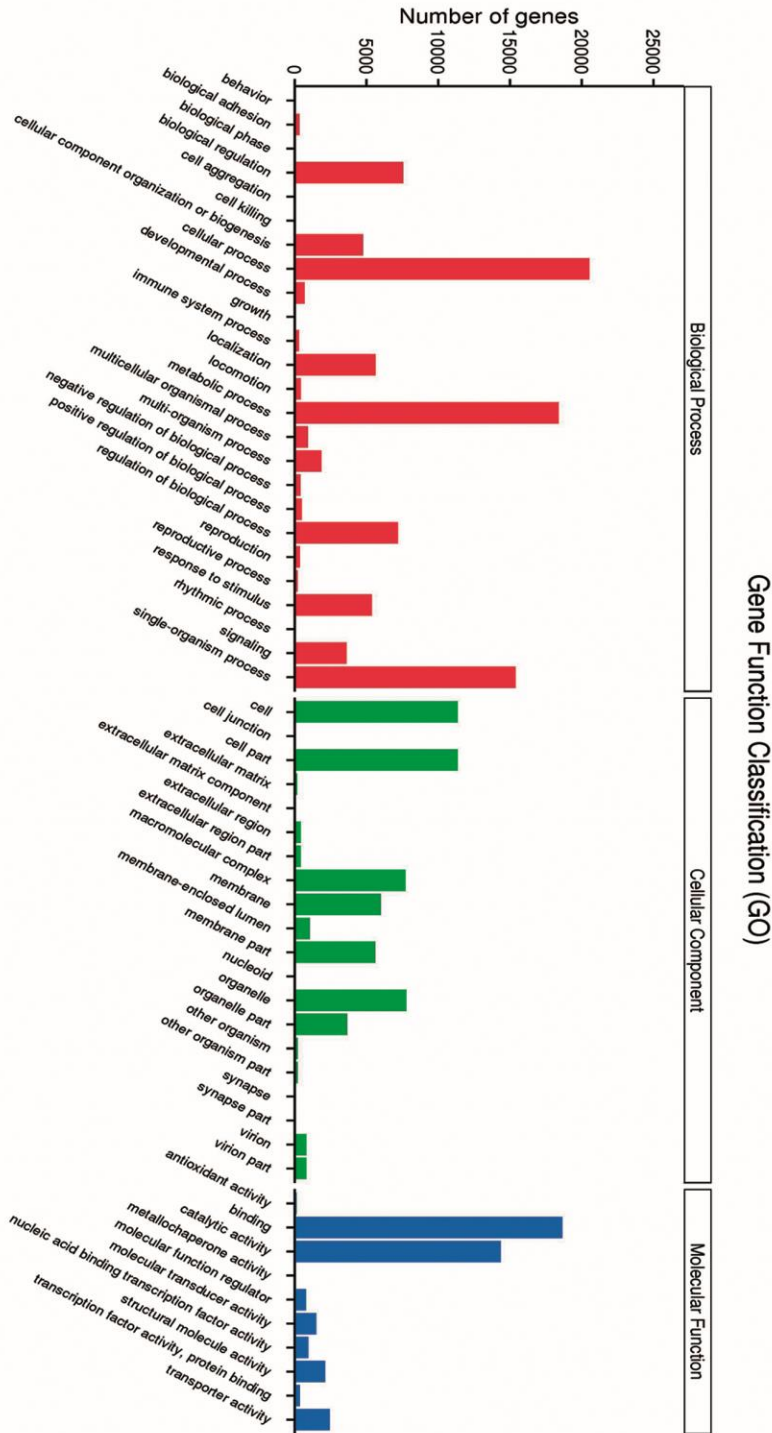


Fig. 3 — Functional annotation of unigenes based on gene ontology

Differentially expressed genes

A total of 202 genes were differentially expressed between the SP and HP groups, and 417 were differentially expressed between the HM and SM groups. Seventy genes were differentially expressed in both comparisons (Fig. 6).

GO enrichment analysis of differentially expressed genes

Genes differentially expressed between the HP and SP groups were significantly enriched in the category of biological process, associated with DNA replication initiation and tetrapyrrole metabolic process. Genes differentially expressed between the

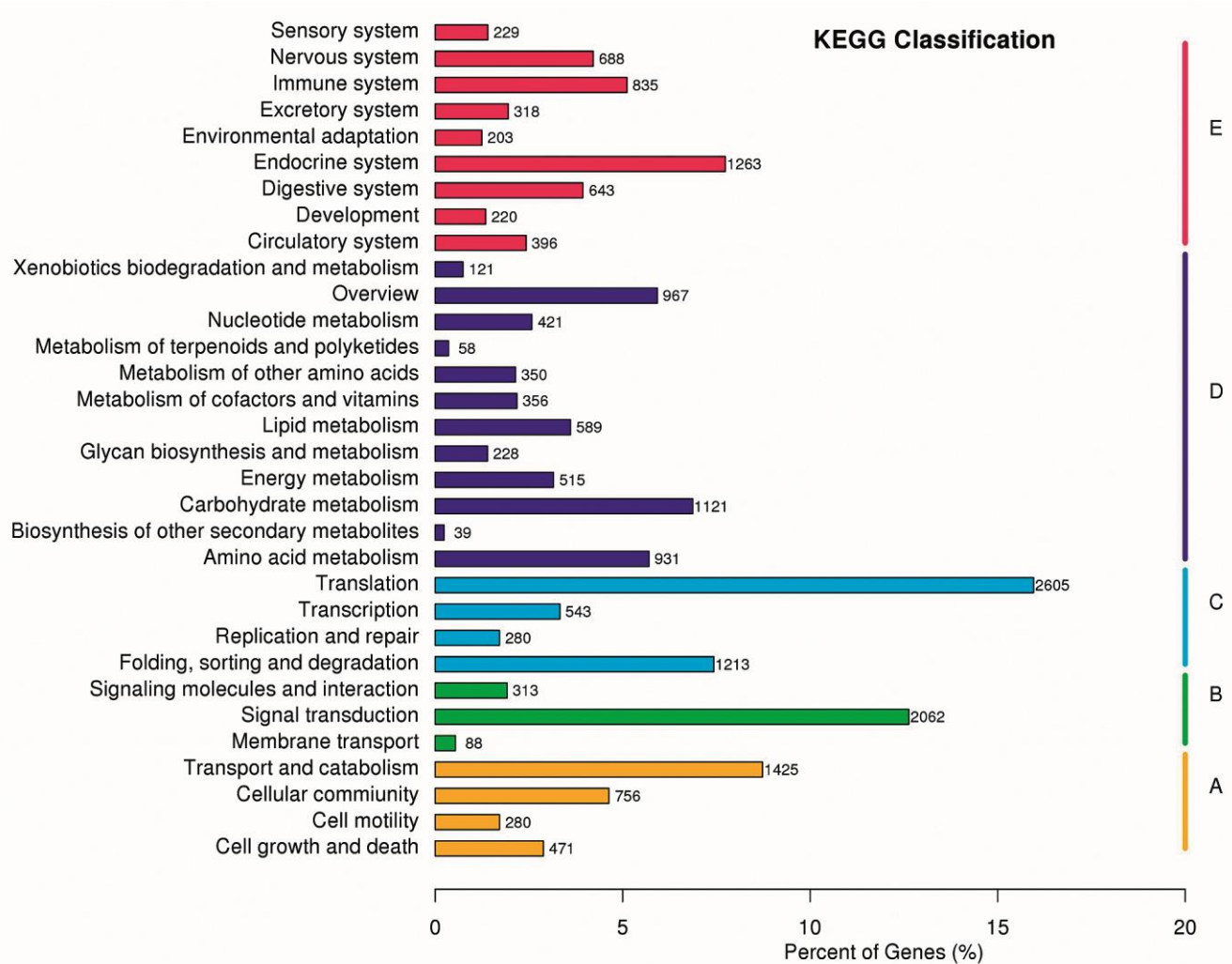


Fig. 4 — KEGG classification (a: Cellular processes; b: Environmental information processing; c: Genetic information processing; d: Metabolism; and e: Organismal systems)

HM and SM groups were significantly enriched in biological process, cell component and molecular function. Eighty-three differentially expressed genes were related to protein metabolic process and 45 were associated with proteolysis in the biological process category, 15 were related to extracellular matrix in the cell component category and most differentially expressed genes in the molecular function category were related to peptidase activity (Fig. 7).

KEGG enrichment analysis of differentially expressed genes

Genes differentially expressed between the HP and SP groups were enriched in mineral absorption, protein digestion and absorption, HIF-1 signalling pathway, and glycolysis/gluconeogenesis. Genes differentially expressed between the HM and SM groups were enriched in protein digestion and absorption, PPAR signalling pathway and HIF

signalling pathway (Fig. 8). Genes that were differentially expressed between both comparisons were enriched in protein digestion and absorption and the HIF signalling pathway, while glycolysis/gluconeogenesis and mineral absorption-related genes only appeared in the HP vs SP comparison.

Differentially expressed genes involved in protein digestion and absorption in the HP vs SP sample group were down-regulated, including collagen and carboxypeptidase A1 genes. In contrast, differentially expressed genes involved in mineral absorption, HIF signalling pathway, and glycolysis/gluconeogenesis were up-regulated, including genes for heme oxygenase, transferrin and zinc transporter involved in mineral absorption, Prolyl Hydroxylase Domain (PHD) and transferrin involved in HIF signalling pathway, fructose-bisphosphate aldolase (ALDOA),

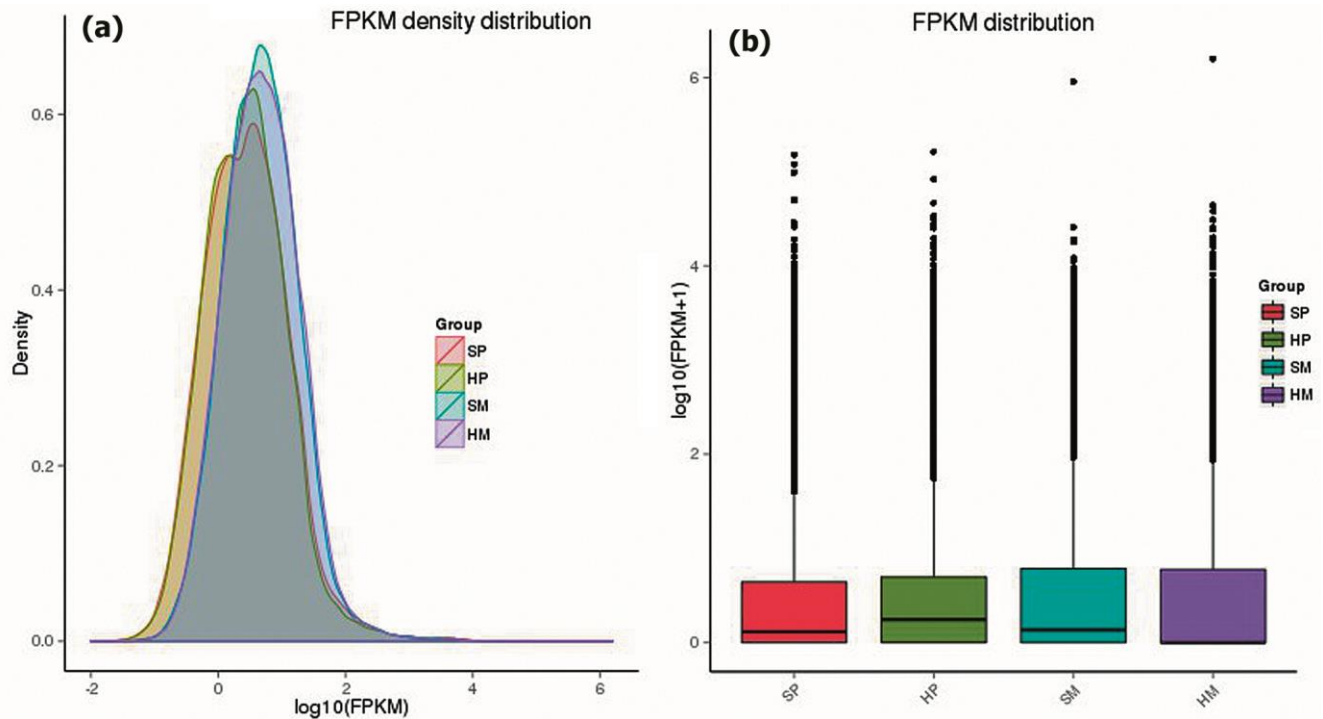


Fig. 5 — Analysis of gene expression in four samples: (a) FPKM density distribution; and (b) FPKM distribution

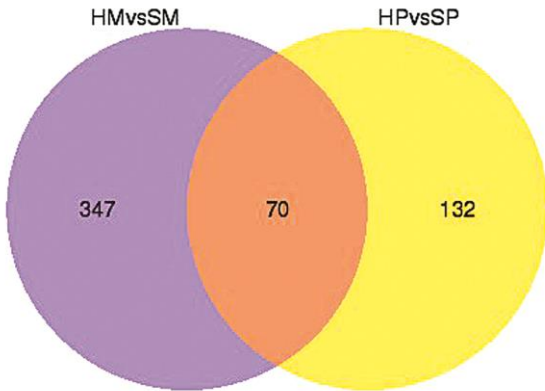


Fig. 6 — The number of differential expression genes in two groups

fructose-1,6-bisphosphatase (FBP), phosphoglucomutase (PGM), and phosphoenolpyruvate carboxykinase (PCK) involved in glycolysis/gluconeogenesis, and Nicotinamide adenine dinucleotide (NADH) dehydrogenase involved in oxidative phosphorylation.

Similar to the HP vs SP sample group, differentially expressed genes in the HM vs SM sample group involved in protein digestion and absorption were down-regulated, including collagen, neprilysin, chymotrypsin-like protease, pancreatic elastase II, and carboxypeptidase A1 genes, while differentially expressed genes involved in HIF

signalling were significantly up-regulated, including genes encoding PHD, HIF-1 β and its binding protein CBP/p300, and ubiquitin-protein ligase E3. Expression of genes encoding heme oxygenase, ALDO, NADH dehydrogenase, and cytochrome c oxidase involved in oxidative phosphorylation, as well as some genes related to the proper folding, sorting, and transport of proteins in the endoplasmic reticulum, such as HYOU1, HSP70, and protein transport protein (SEC61), were also up-regulated. AP1 gene expression was also significantly up-regulated.

Expression and verification of key genes

We analyzed the fold-change differences in gene expression levels of collagen, PHD, transferrin, HIF1 β , binding protein CBP/p300, heme oxygenase, ALDO, NADH dehydrogenase, cytochrome c oxidase, HSP70, and AP1 (Fig. 9). Expression levels of related genes were compared between medusae and between polyps after cultivation for 18h under hypoxic and normoxic conditions. In the HIF signalling pathway, PHD gene expression was induced by hypoxia in both medusae (relative expression level 202.3) and polyps (58.9), while HIF-1 β and CBP/p300 genes were significantly induced by hypoxia in medusae (15.3 and 2.9, respectively), but not in polyps. Gene expression levels of ALDO and

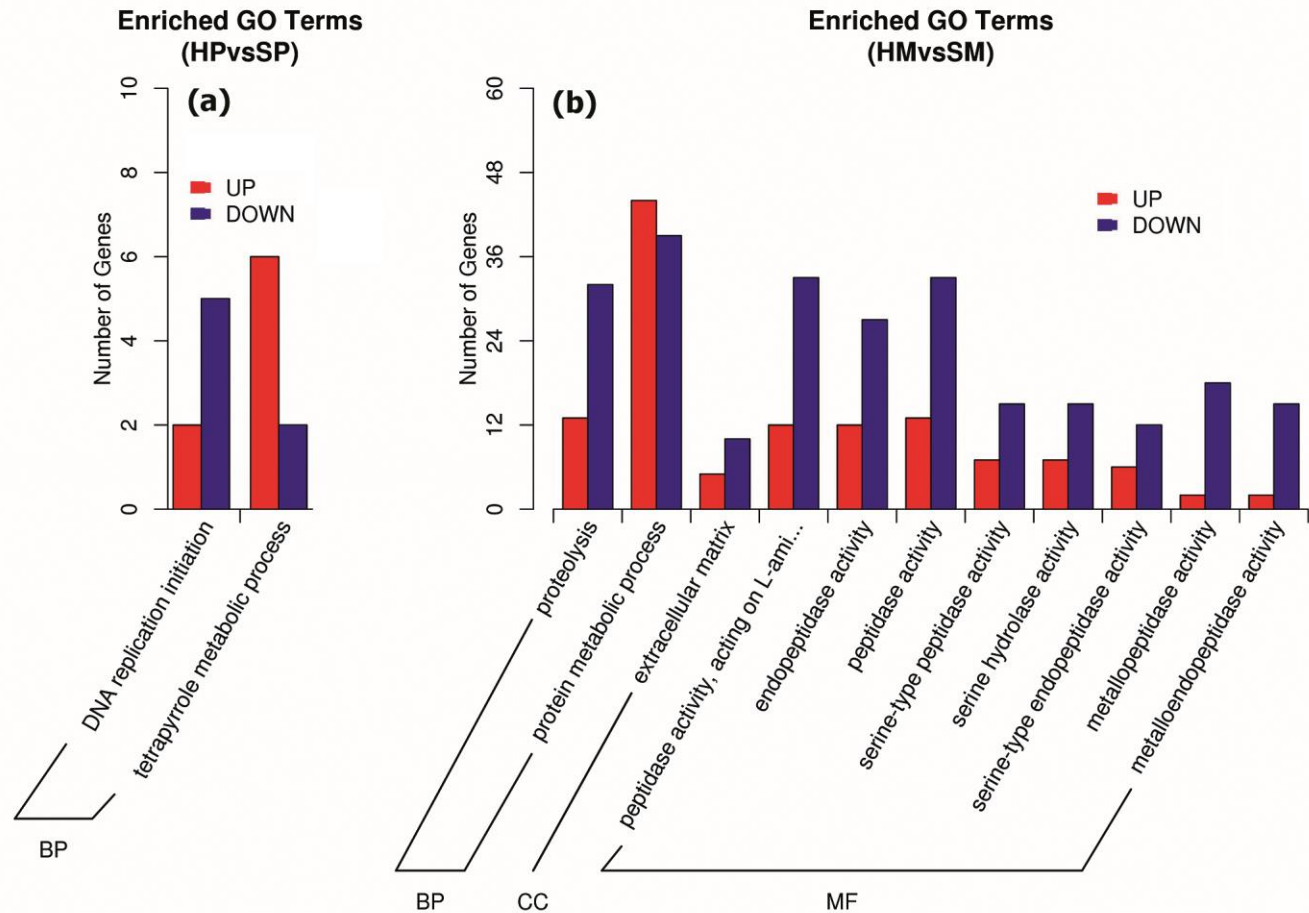


Fig. 7 — GO annotation of differential expression genes: BP: biological process; CC: cellular component; and MF: molecular function [(a) HP vs SP; and (b) HM vs SM]

NADH dehydrogenase, involved in the process of glycolysis and oxidative phosphorylation, were significantly induced by hypoxia in both medusae and polyps; cytochrome c oxidase was significantly increased in medusae (21.8), but not in polyps; heme oxygenase and transferrin genes were significantly induced by hypoxia in both medusae and polyps, while the HSP70 gene was significantly induced by hypoxia in medusae (29.2) but not in polyps. Similarly, AP1 was significantly induced by hypoxia in medusae (2.9) but not in polyps. The collagen gene was significantly down-regulated by hypoxia in both medusae and polyps (relative expression levels 0.38 and 0.47, respectively).

The expression of the above genes was verified by RT-qPCR, which showed that HIF-1 β , CBP/p300, ALDO, NADH dehydrogenase, cytochrome c oxidase, heme oxygenase, transferrin, and HSP70 genes were significantly up-regulated in both medusae and polyps, while the difference in

expression levels of the PHD and collagen genes in polyps was not significant, and the AP1 gene was significantly down-regulated in polyps.

The expression results for the key genes quantified by RNA-Seq were consistent with the results of RT-qPCR in medusae, but the gene expression results for PHD, HIF-1 β , CBP/p300, cytochrome c oxidase, HSP70, AP1, and collagen in polyps differed between RNA-Seq and RT-qPCR.

Discussion

In this study, we sequenced the transcriptome of the moon jellyfish *A. coerulea* and performed *de novo* transcriptome assembly. We identified 138,945 unigenes and annotated them using seven databases; however, only 40.1 % of unigenes were annotated in these databases. We carried out transcriptome sequencing of different life cycle stages of jellyfish and obtained a total of 131,464 unigenes²³. The numbers of unigenes obtained from the above two

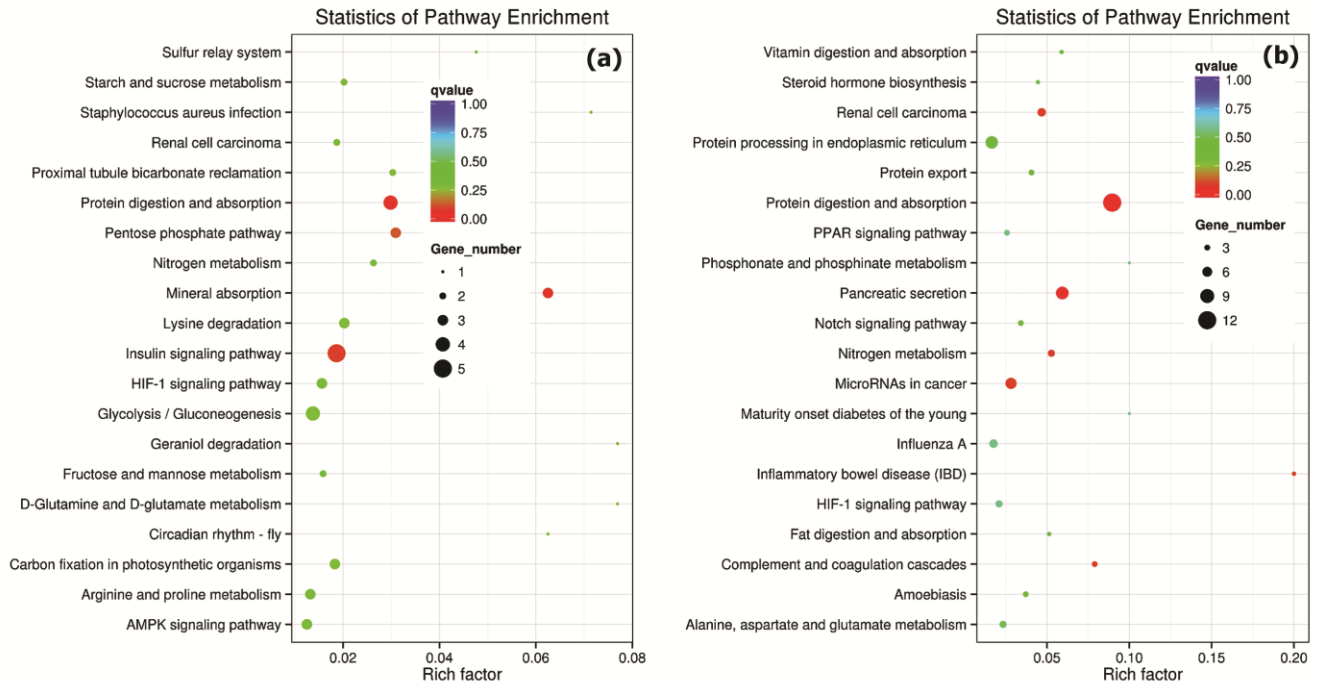


Fig. 8 — Enriched KEGG pathway scatter plot of differential expression genes: (a) HP vs SP; and (b) HM vs SM

transcriptome sequencings were similar, and we did not perform a detailed comparison between the two transcriptome sequences. More than 60 % of the sequences from transcriptome data obtained by Brekman were consistent with the transcriptome sequences obtained by Fuchs²⁴. Differences may exist between transcriptome sequences for the same species, depending on the sequencing depth and assembly techniques. The low rate of transcriptome annotation in the current study may have been because of the small number of gene sequences for moon jellyfish in the databases, together with large nucleic acid sequence variation during jellyfish evolution. Only 17.1 % of unigenes were mapped to *H. vulgaris* in the same phylum Cnidaria.

A total of 619 differentially expressed genes were obtained by comparing gene expression levels between jellyfish under hypoxic and normoxic conditions, including 417 differentially expressed genes in medusae and 202 in polyps. These differentially expressed genes were enriched in processes of HIF signalling pathway, oxidative phosphorylation, mineral absorption, and protein digestion and absorption, with differences in the number of differentially expressed genes enriched in the above signalling pathways between the two different life stages. In addition, differentially expressed genes were only associated with the

gluconeogenesis signalling pathway in polyps, and with protein folding, sorting and transport in the endoplasmic reticulum in medusae.

PHD was the only differentially expressed gene enriched in the HIF signalling pathway in polyps, while PHD, HIF-1 β , and CBP/p300 were differentially expressed in medusae. The expression of PHD, as an oxygen sensor factor in cells, was significantly induced by hypoxia. HIF-1 β , also known as aryl hydrocarbon receptor nuclear translocator, forms a transcription factor dimer with HIF-1 α , and the dimer associated with CBP/p300 binds to the hypoxia-response elements of the target genes to induce their expression. HIF-1 α gene transcription was significantly induced by hypoxia in jellyfish¹², and expression of the HIF-1 α gene was also significantly up-regulated after hypoxia treatment in human CD4⁺ T cells²⁵. In the current study, HIF-1 α gene expression was up-regulated to a certain extent according to FPKM, but the difference was not significant according to DEGseq because of insufficient biological replicates. Downstream target genes of the HIF signalling pathway include transferrin, heme oxygenase, and ALDO. Transcriptome sequencing of the fish *Oligocottus maculosus* found that glycolysis was the main physiological process involved in the response to hypoxia¹⁸. ALDO is a key rate-limiting enzyme in the

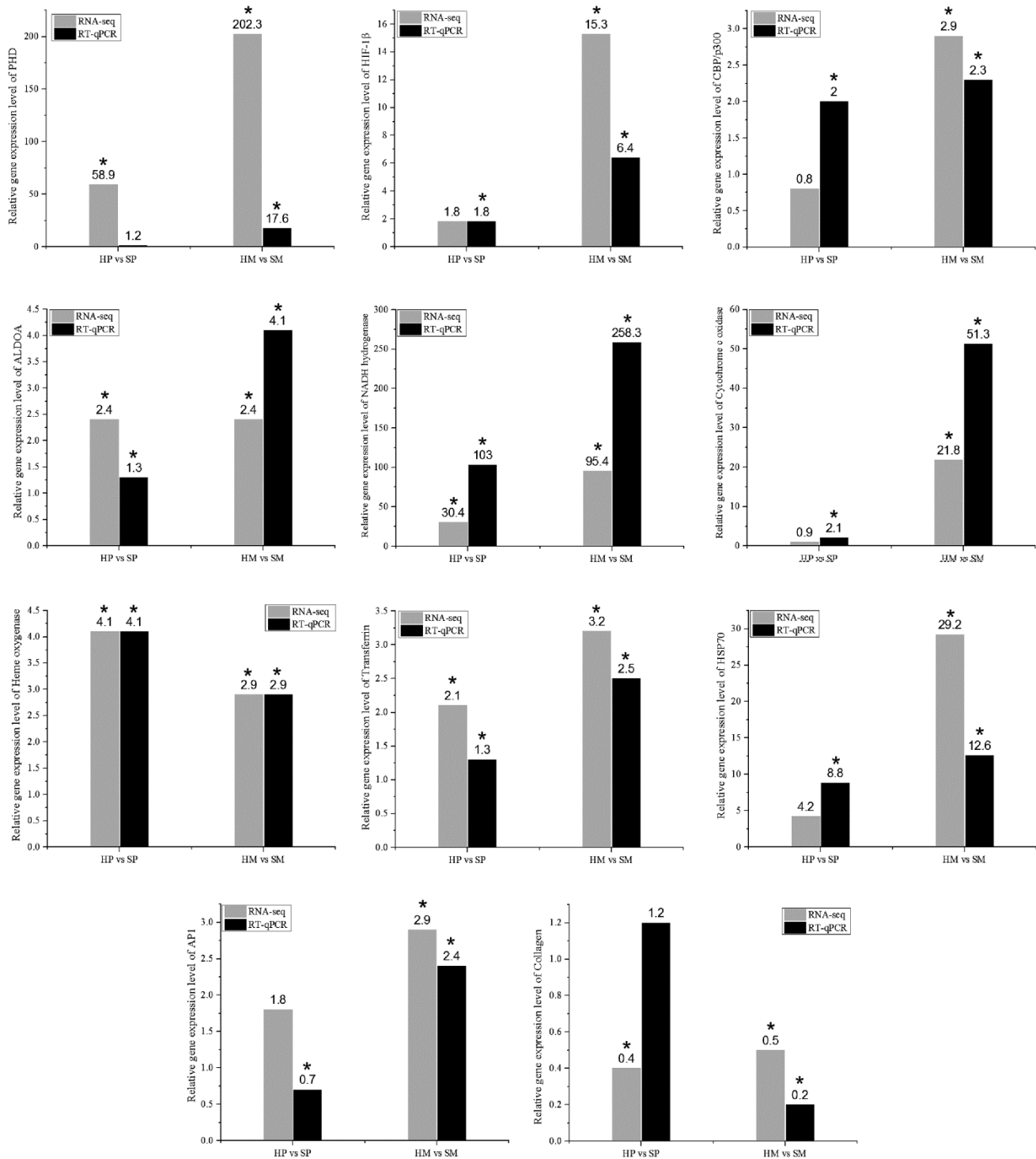


Fig. 9 — The relative expression of key genes (* represents $p < 0.05$)

glycolytic process, and it's up-regulation accelerates the glycolytic process to generate more ATP and reduce reactive oxygen species. Transferrin and heme oxygenase participate in the synthesis of hemoglobin

in higher animals and increase the oxygen-carrying capacity of the circulatory system. Moon jellyfish have not evolved a circulatory system, but transcriptome annotation revealed the presence of

hemoglobin-like sequences such as flavohemoglobin, group 1 truncated hemoglobin, and non-symbiotic hemoglobin 1 and 2. Oxygen in cells acts as an electron acceptor and is directly involved in the respiratory electron transport chain, which produces the energy needed by the cells. Transcriptome sequencing of *Aspergillus fumigatus* after hypoxia induction identified cellular respiration as a key process affecting survival under hypoxic conditions²⁶. Oxidative phosphorylation and the respiratory electron transport chain are key processes in aerobic metabolism. NADH dehydrogenase is an enzyme located on the inner mitochondrial membrane, which catalyzes the transfer of electrons from NADH to coenzyme Q²⁷. It controls the inlet of oxidative phosphorylation in mitochondria, providing electrons for the reduction of oxygen molecules. Cytochrome oxidase is the last enzyme in the electron transport chain and acts as a proton pump that actively transports H⁺ from the matrix to the intermembrane space, while also transferring electrons to oxygen to form water through redox changes in heme iron and copper present in the protein²⁸. Expression levels of these two genes were up-regulated under hypoxic conditions to counteract the lack of oxygen and produce energy to maintain cell survival²⁹. Expression levels of genes involved in protein folding, sorting and transport in the endoplasmic reticulum, such as HSP70 and Sec61, were also significantly up-regulated in medusae, compared with polyps, under hypoxic conditions. Protein folding and trafficking were also involved in the response to hypoxia in human CD4⁺ T cells²⁵. HSP70 participates in protein folding and maintains protein stability in cells, and is often used as a molecular marker for stress. Sec61 is a transporter responsible for the export of proteins from the endoplasmic reticulum³⁰, and studies have shown that Sec61 is also involved in the formation of Ca²⁺ channels in the endoplasmic reticulum. HSP70 gene expression was shown to be up-regulated by hypoxic stress, while the underlying mechanism of Sec61 gene expression in response to hypoxia remains to be further studied. AP1 transcription was significantly induced by hypoxia in medusae, but not in polyps. AP1 acts as a transcription factor to regulate the expression of target genes in response to external stimuli (cytokines, growth factors, stress, bacterial and viral infections, etc.), and participates in various cellular processes, including differentiation, proliferation, and apoptosis³¹. Under hypoxia, the stress signal may be transduced to the transcription

factor AP1 via the JNK signalling pathway in medusae, and in the absence of energy, AP1 may initiate programmed apoptosis by up-regulating the expression of the appropriate target genes. The JNK signalling and HIF signalling pathways may thus interact in response to hypoxia.

Analysis of differentially expressed genes and transcriptome functional gene annotation identified a hemoglobin-like gene in jellyfish. Although the function of the gene expression product in lower animals remains indistinct, it may signify the basis for subsequent hemoglobin evolution in higher animals, or may already possess an oxygen-binding capacity similar to that in higher animals. Further studies are recommended to sightsee this in more depth.

In addition, the significant up-regulation of AP1 transcription in medusae suggests that hypoxic stress may lead to the death of organisms via an interaction between the HIF and JNK signalling pathways, as well as providing a baseline for the study of the responses of jellyfish to external stress, while there is scarce of established research of jellyfish in this area for further discussion.

Conclusion

A total of 138,945 unigenes were obtained by transcriptome sequencing and *de novo* assembly in the moon jellyfish, *Aurelia coerulea*. However, only 40.1 % of these unigenes were annotated in seven databases. A comparison of gene expression levels under hypoxic and normoxic conditions revealed 619 differentially expressed genes, including 417 in medusae and 202 in polyps, which were enriched in HIF signalling pathway, oxidative phosphorylation, mineral absorption, and protein digestion and absorption. These results suggest that moon jellyfish acquire tolerance to hypoxic environments through down-regulating the expression of genes related to protein digestion and absorption and up-regulating the expression of genes related to HIF signalling pathway, glycolysis, oxidative phosphorylation, pyrrole metabolism, mineral absorption, and protein folding, sorting, and transport.

Supplementary Data

Supplementary data associated with this article is available in the electronic form at [http://nopr.niscpr.res.in/jinfo/ijms/IJMS_51\(02\)138-151_SupplData.pdf](http://nopr.niscpr.res.in/jinfo/ijms/IJMS_51(02)138-151_SupplData.pdf)

Acknowledgements

The authors thank Zhang Fang, Associate Research Fellow of the Institute of Oceanology, Chinese Academy of Sciences, for providing medusae and polyps of *A. coerulea*. This work was supported by the National Key Research and Development Program of China (No. 2017YFC1404406), the National Natural Science Foundation of China (No. 41606135) and the Open Research Fund Program of Guangxi Key Lab of Mangrove Conservation and Utilization (No. GKLMC-201402).

Conflict of Interest

The authors declare that they have no financial and personal relationship with other people or organizations that can inappropriately influence on this manuscript.

Author Contributions

GW designed the study, contributed in reagents/materials/ analysis tools and wrote the manuscript draft; YX performed tissue collection, RNA isolation, performed the RT-qPCR experiments; GW & YX performed the data analysis, edited the manuscript. Both the authors have approved the manuscript.

References

- Scorrano S, Aglieri G, Boero F, Dawson M N & Piraino S, Unmasking *Aurelia* species in the Mediterranean Sea: an integrative morphometric and molecular approach, *Zool J Linn Soc-Lon*, 180 (2016) 243–267.
- Richard A H & Purcell J E, Substrate preferences of scyphozoan *Aurelia labiate* polyps among common dock-building materials, *Hydrobiologia*, 616 (2009) 259–267.
- Purcell J E, Jellyfish and ctenophore blooms coincide with human proliferations and environmental perturbations, *Annu Rev Mar Sci*, 4 (2012) 209–235.
- Vaquer-Sunyer R & Duarte C M, Thresholds of hypoxia for marine biodiversity, *Proc Natl Acad Sci*, 105 (2008) 15452–15457.
- Shoji J, Masuda R, Yamashita Y & Tanaka M, Effect of low dissolved oxygen concentrations on behavior and predation rates on red sea bream *Pagrus major* larvae by the jellyfish *Aurelia aurita* and by juvenile Spanish mackerel *Scomberomorus niphonius*, *Mar Biol*, 147 (2005) 863–868.
- Shoji J, Masuda R, Yamashita Y & Tanaka M, Predation on fish larvae by moon jellyfish *Aurelia aurita* under low dissolved oxygen concentrations, *Fisheries Sci*, 71 (2005) 748–753.
- Shoji J, Non-size-selective predation on fish larvae by moon jellyfish *Aurelia aurita* under low oxygen concentrations, *Plankton Benthos Res*, 3 (2008) 114–117.
- Ishii H, Ohba T & Kobayashi T, Effects of low dissolved oxygen on planula settlement polyp growth and asexual reproduction of *Aurelia aurita*, *Plankton Benthos Res*, 3 (2008) 107–113.
- Rytkönen K T & Storz J F, Evolutionary origins of oxygen sensing in animals, *EMBO Rep*, 12 (2011) 3–4.
- Wang G, Zhen Y, Wang M, Wang J, Shi Y, *et al.*, Hypoxia induced gene expression under acute hypoxic stress in *Aurelia* sp. 1, *Chinese Sci Bull*, 59 (2014) 1715–1722.
- Wang G, Yu Z, Zhen Y, Mi T, Shi Y, *et al.*, Molecular characterisation, evolution and expression of hypoxia-inducible factor in *Aurelia* sp. 1, *Plos One*, 9 (6) (2014) e100057.
- Wang G, Zhen Y, Yu Z, Shi Y, Zhao Q, *et al.*, The physiological and molecular response of *Aurelia* sp. 1 under hypoxia, *Sci Rep*, 7 (2017) p. 1558.
- Vidal-Dupiol J, Zoccola D, Eric Tambutté, Grunau C, Céline Cosseau, *et al.*, Genes related to ion-transport and energy production are upregulated in response to CO₂-driven pH decrease in corals: new insights from transcriptome analysis, *Plos One*, 8 (3) (2013) e58652.
- Elran R, Raam M, Kraus R, Brekhman V, Sher N, *et al.*, Early and late response of *Nematostella vectensis* transcriptome to heavy metals, *Mol Ecol*, 23 (2014) 4722–4736.
- Diaz R J & Rosenberg R, Spreading dead zones and consequences for marine ecosystems (Review), *Science*, 321 (2008) 926–929.
- Liao X, Cheng L, Xu P, Lu G, Wachholtz M, *et al.*, Transcriptome analysis of crucian carp (*Carassius auratus*), an important aquaculture and hypoxia-tolerant species, *Plos One*, 8 (4) (2013) e62308.
- Wang Y, Yang L, Wu B, Song Z & He S, Transcriptome analysis of the plateau fish (*Triplophysa dalaica*): Implications for adaptation to hypoxia in fishes, *Gene*, 565 (2015) 211–220.
- Mandic M, Ramon M L, Gracey A Y & Richards J G, Divergent transcriptional patterns are related to differences in hypoxia tolerance between the intertidal and the subtidal sculpins, *Mol Ecol*, 23 (2014) 6091–6103.
- Tiedke J, Borner J, Beeck H, Kwiatkowski M, Schmidt H, *et al.*, Evaluating the hypoxia response of ruffe and flounder gills by a combined proteome and transcriptome approach, *Plos One*, 10 (8) (2015) e0135911.
- Schroth W, Ender A & Schierwater B, Molecular biomarkers and adaptation to environmental stress in moon jelly (*Aurelia* spp.), *Mar Biotechnol*, 7 (2005) 449–461.
- Grabherr M G, Haas B J, Yassour M, Levin J Z, Thompson D A, *et al.*, Full-length transcriptome assembly from RNA-seq data without a reference genome, *Nat Biotechnol*, 29 (2011) 644–652.
- Li B & Dewey C, RSEM: accurate transcript quantification from RNA-Seq data with or without a reference genome, *BMC Bioinformatics*, 12 (2011) 323.
- Brekhman V, Malik A, Haas B, Sher N & Lotan T, Transcriptome profiling of the dynamic life cycle of the Scyphozoan jellyfish *Aurelia aurita*, *BMC Genomics*, 16 (2015) 1–14.
- Fuchs B, Wang W, Graspentner S, Li Y, Insua S, *et al.*, Regulation of polyp-to-jellyfish transition in *Aurelia aurita*, *Curr Biol*, 24 (2014) 263–273.

- 25 Gaber T, Haupl T, Sandig G, Tykwinska K, Fangradt M, *et al.*, Adaptation of human cd4+ t cells to pathophysiological hypoxia: a transcriptome analysis, *J Rheumatol*, 36 (2009) 2655–2669.
- 26 Kroll K, Pahtz V, Hillmann F, Vaknin Y, Schmidt-Heck W, *et al.*, Identification of hypoxia-inducible target genes of *Aspergillus fumigatus* by transcriptome analysis reveals cellular respiration as an important contributor to hypoxic survival, *Eukaryot Cell*, 13 (2014) 1241–1253.
- 27 Schomburg D, Salzmann M & Stephan D, NADH dehydrogenase (ubiquinone), In: *Enzyme Handbook*, 7, edited by Schomburg D, Salzmann M & Stephan D, (Springer, Berlin, Heidelberg), 1994, pp. 293–302.
- 28 Fukuda R, Zhang H, Kim J W, Shimoda L, Dang C V, *et al.*, HIF-1 regulates cytochrome oxidase subunits to optimize efficiency of respiration in hypoxic cells, *Cell*, 129 (2007) 111–122.
- 29 Tan X, Liu J-Z, Cao L-F, Deng Z-C & Li Y-H, Effects of hypoxic exposure on coordinative expression of cytochrome oxidase subunits I and IV in rat cerebral cortex, *Acta Physiol Sin*, 54 (2002) 529–524.
- 30 Park E, Ménétret J F, Gumbart J C, Ludtke S J, Li W, *et al.*, Structure of the secY channel during initiation of protein translocation, *Nature*, 506 (7486) (2014) 102–106.
- 31 Lopez-Bergami P, Lau E & Ronai Z, Emerging roles of ATF2 and the dynamic AP1 network in cancer, *Nat Rev Cancer*, 10 (2010) 65–76.